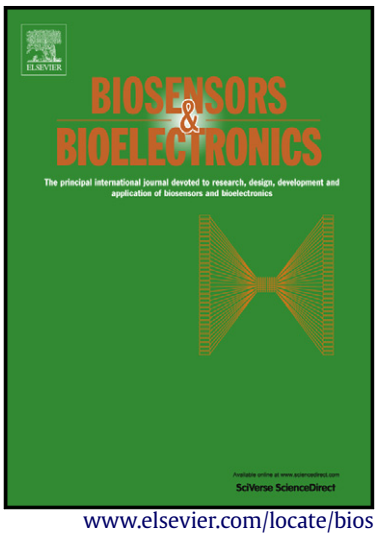

www.elsevier.com/locate/bios

Label-free and Reagentless Electrochemical Detection of micro RNAs using a Conducting Polymer Nanostructured by Carbon Nanotubes. Application to Prostate Cancer Biomarker miR-141

H.V. Tran, B. Piro, S. Reisberg, L.D. Tran, H.T. Duc, M.C. Pham

PII: S0956-5663(13)00321-7
DOI: http://dx.doi.org/10.1016/j.bios.2013.05.007
Reference: BIOS5935

To appear in: *Biosensors and Bioelectronics*

Received date: 4 February 2013
Revised date: 12 April 2013
Accepted date: 2 May 2013

Cite this article as: H.V. Tran, B. Piro, S. Reisberg, L.D. Tran, H.T. Duc, M.C. Pham, Label-free and Reagentless Electrochemical Detection of micro RNAs using a Conducting Polymer Nanostructured by Carbon Nanotubes. Application to Prostate Cancer Biomarker miR-141, *Biosensors and Bioelectronics,* http://dx.doi.org/10.1016/j.bios.2013.05.007

Label-free and Reagentless Electrochemical Detection of micro RNAs using a Conducting Polymer Nanostructured by Carbon Nanotubes. Application to Prostate Cancer Biomarker miR-141.

H. V. Tran[1,2], B. Piro[1], S. Reisberg[1], L.D. Tran[3], H.T. Duc[4], M.C. Pham[1*]

[1] *Univ. Paris Diderot, Sorbonne Paris Cité, ITODYS, UMR 7086 CNRS, 15 rue J-A de Baïf, 75205 Paris Cedex 13, France*

[2] *USTH ,University of Science and Technology of Hanoi, 18 Hoang Quoc Viet, Hanoi, Vietnam*

[3] *Institute of Material Sciences (IMS), Vietnamese Academy of Science and Technology, 18 Hoang Quoc Viet, Hanoi, Vietnam*

[4] *Université Paris XI, INSERM U-1014, Groupe Hospitalier Paul Brousse-94800 Villejuif, France*

Abstract

In this paper, a label-free and reagentless microRNA sensor based on an interpenetrated network of carbon nanotubes and electroactive polymer is described. The nanostructured polymer film presents very well-defined electroactivity in neutral aqueous medium in the cathodic potential domain from the quinone group embedded in the polymer backbone. Addition of microRNA miR-141 target (prostate cancer biomarker) gives a "signal-on" response, i.e. a current increase due to enhancement of the polymer electroactivity. On the contrary, non-complementary miRNAs such as miR-103 and miR-29b-1 do not lead to any significant current change. A very low detection limit of ca. 8 fM is achieved with this sensor.

Keywords: Conducting polymer; Square wave voltammetry; Oligonucleotides; Electrochemical biosensor; Label-free detection; microRNA.

* Corresponding author. Tel. +33-1-57277223. Email: mcpham@univ-paris-diderot.fr

Introduction

The biology of the late 20th century was marked by the discovery in 1993 of a new class of small non-coding ribonucleic acids (RNAs) which play major roles in regulating the translation and degradation of messenger RNAs (Lee et al., 1993; Wightman et al., 1993). These small RNAs (18-25 nucleotides), called microRNAs (miRNA), are implied in several biological processes such as differentiation, metabolic homeostasis, cellular apoptosis and proliferation (Iorio and Croce, 2009; Brase et al., 2010).

The discovery in 2008 that the presence of miRNAs in body fluid is in correlation with cancer (prostate, breast, colon, lung, …) or other diseases (diabetes, heart diseases, …) has made them new key players as biomarkers (Lawrie et al., 2008; Catuogno et al., 2011, Chen et al., 2008). Actually, more than 1200 miRNAs have been identified (Liu et al., 2012), among which miR-141 is detected at elevated level in blood of patients having metastatic prostate cancer (Mitchell et al., 2008).

Current standard methods for identification and quantification of miRNAs are based on traditional molecular biology techniques (Northern blot, microarray, qRT-PCR). These approaches although very sensitive and reliable are often expensive, time consuming, and need highly trained technicians (Hunt et al., 2009; Planell-Saguer and Rodicio, 2011). That's why a real challenge is to develop devices able to detect and quantify easily and simultaneously different miRNA sequences at sub-picomolar levels (Wang et al., 2012). Ideally, these new bioanalytical tools should be easy to manufacture, need low power, and allow reagentless and label-free detection . Few work deal with such strategy, and particularly very few when electrochemical transduction is involved. Electrochemical biosensors offer the advantages of mass fabrication, low cost and potential decentralized analysis (Paleček and Bartošík, 2012).

Lusi et al.,(2009) reported amperometric detection based on oxidation of RNA nucleobases This system allows detection at sub-picomolar level (0.1 pM) but the current depends on the number of guanine and needs high oxidation potentials, which may generate side-oxidations. Using enzyme-labeled detection probes, Kilic et al. (2012) reported detection for miR-21 with a detection limit of 1 μM. Gao et al. (2011) achieved a detection limit of 10 fM. Allosteric molecular beacons able to bind HRP enzyme were used by Cai et al. (2013), with a detection limit of 44 amol in a volume of 4 μL, i.e. 11 pM. Yin et al. (2012) have shown a detection limit of 60 fM for miR-21 with gold NPs bearing HRP. Using a polymerase-labeled DNA probe and impedance measurements, Shen et al. (2013) reported a LOD of 2 fM for a S/N of 3. Very high sensitivity (0.1 fM) was obtained using peptide nucleic acid (PNA) probes (Zhang et al., 2009). Qavi et al., 2010, proposed an excellent review on miRNA analysis.

Conducting polymers constitute a powerful platform to immobilize short DNA or RNA sequences while maintaining their stability, accessibility and activity (Gerard et al., 2002; Cosnier et al., 2003; Cosnier, 1999). Unfortunately, label-free electrochemical biosensors based on polymer-modified electrodes are known to suffer from lack of sensitivity (Cosnier and Holzinger, 2011). To enhance sensitivity, carbon nanotubes (CNTs) were frequently reported (Wohlstadter et al., 2003; Wang et al., 2005) to increase the electroactive area and decrease the electrical resistance of the working electrodes, leading to 3D conductive materials (Peigney et al., 2001; Kulesza et al., 2006; Acevedo et al., 2008). Qi et al., (2007) fabricated an electrochemical DNA biosensor based on electropolymerised polypyrrole and carbon nanotubes, using ethidium bromide as redox indicator with high sensitivity, ca. 85 pM. Very few works were related to label-free and reagentless biosensors.

Okuno et al., (2007) described a label-free and reagentless immunosensor for prostate-specific antigen based on single-walled CNT-modified microelectrodes with low detection limit (0.25 ng mL^{-1}). The current being derived from oxidation of amino acid residues (tyrosine and

tryptophan), it is then dependent on the presence of these residues in the target sequence. Zhang et al., (2011) described a strategy for label-free and reagentless electrochemical DNA sensing based on SWNTs and an immobilized redox probe. This system allows very specific detection of DNA but the limit of detection is only 0.1 μM. 3D structures obtained using CNTs may induce high capacitance which may introduce distortion on cyclic voltammograms (Peng et al., 2007). In order to minimize this effect, pulsed methods such as differential pulse voltammetry (DPV) or square wave voltammetry (SWV) are currently used. Impedance methods combining polymer and carbon nanotubes have also been widely used in reagentless formats (Xu et al., 2004, 2006; Cai et al., 2003). In this paper, we describe a label-free and reagentless miRNA sensor based on an interpenetrated network of carbon nanotubes and electroactive polymer. The nanostructured polymer film presents very well-defined electroactivity in neutral aqueous medium from the quinone group embedded in the polymer backbone. When the miRNA-141 target is added (miR-141, a prostate biomarker) a "signal-on" response, i.e. a current increase, is observed while no current change occurs with non-complementary miRNAs such as miR-103 (a colorectal cancer biomarker; Chen et al., 2012) or miR-29b-1 (a lung cancer biomarker; Fabbri et al., 2007). The biosensor presents a very low detection limit of ca. 8 fM.

1. Experimentals

2.1. Chemicals

Phosphate buffer saline (PBS, 0.137 M NaCl; 0.0027 M KCl; 0.0081 M Na_2HPO_4; 0.00147 M KH_2PO_4, pH 7.4) was provided by Sigma. Aqueous solutions were made with ultrapure (18 MΩ cm) water. Glassy carbon (GC) working electrodes (3 mm diameter, S = 0.07 cm^2) were purchased from BASInc. 3-(5-hydroxy-1,4-dioxo-1,4-dihydronaphthalen-2(3)-yl) propanoic acid (JUGA) was synthesized from 5-hydroxy-1,4-naphthoquinone (JUG) and

succinic acid (Piro et al., 2011). All oligonucleotides were provided by Eurogentec (Belgium). All sequences are detailed in Table 1. DNA strands were used as capture probes for the corresponding miRNAs. Human sera were provided by Paul Brousse Hospital (H.T. Duc). Multi-walled carbon nanotubes (MWCNTs, purity 90%; diameter of 110 - 170 nm and length of 5 - 9 µm), lithium perchlorate (purity ≥ 95%) and 5-hydroxy-1,4-naphthoquinone (JUG, purity 97%) were purchased from Sigma Aldrich. 1-(3-dimethylaminopropyl)-3-ethylcarbodiimide hydrochloride (EDC, purity 98%) and N-hydroxysuccinimide (NHS, purity 98%) were from Alfa Aesar (Ward Hill, MA). Alumina slurry is from ESCIL, Chassieu, France. All other reagents used (H_2SO_4, HNO_3) and solvents, acetonitrile (ACN), ethanol (EtOH), were PA grade.

[insert Table 1 here, double column]

Table 1. ODN probes and miRNA target sequences

ODN name	Function (type)	Bases	T_m /°C	Sequences
ODN-141-P	Probe (DNA)	22	46.0	5' NH_2 – CCA TCT TTA CCA GAC AGT GTT A 3'
miR-141	Target (RNA)	22	46	3' GGU AGA AAU GGU CUG UCA CAA U 5'
miR-29b-1	Target (RNA)	23	44.8	3' UUG UGA CUA AAG UUU ACC ACG AU 5'
miR-103	Target (RNA)	23	50.2	3'AGU AUC GGG ACA UGU UAC GAC GA 5'

2.2. CNTs preparation

MWCNTs were purified and oxidized in a 1:1 mixture of HNO_3 and H_2SO_4 at 90°C for 1 h, then washed with distilled water until pH 7 and separated by centrifugation. The solid residue was then dried at 80°C for 12 h before use. These oxidized MWCNTs are referred as o-MWCNTs in the following.

2.3. Electrochemical procedures

The three electrodes cell consists of a GC working electrode (3 mm in diameter), a platinum (Pt) grid counter electrode and a commercial calomel electrode (SCE, supplied from Radiometer Analytical). Cyclic voltammetry was used for polymer electrosynthesis, using an Autolab PGSTAT30. Electrochemical Impedance Spectroscopy (EIS) was used for

characterization of the modified electrodes. Impedance spectra were recorded using the FRA module associated with the PGSTAT30 for frequencies between 100 kHz and 100 mHz and a perturbation amplitude of 10 mV. Solutions were systematically deaerated with argon before and during experiments. Field Emission Scanning Electron Microscopy (FESEM) photographs were taken on a Hitachi S4800 system.

2.4. Electrode preparation

GC electrodes were polished by 1 μm alumina slurry on polishing cloth then washed with water, ethanol and ACN in ultrasonic bath for 2 min. 1 mg o-MWCNTs was dispersed in 1 mL H_2O then 5 μL of this solution was dropped onto a freshly polished GC electrode and let dry. This procedure gives CNT-modified electrodes (noted o-MWCNT/GCE) for which the CNT density is controlled by the quantity initially contained in the droplet. GC or o-MWCNT/GCE electrodes were modified by co-electrooxidation of the 2 monomers JUG and JUGA in ACN solution containing 5×10^{-2} M JUG, 3.75×10^{-3} M JUGA, 0.1 M $LiClO_4$ and 10^{-3} M 1-naphthol (the JUGA:JUG ratio is 0.075). This procedure leads to poly(JUG-co-JUGA)-modified electrodes or poly(JUG-co-JUGA)/o-MWCNT-modified electrodes.

2.5. Grafting ODN capture probes

Poly(JUG-co-JUGA)-modified electrodes or poly(JUG-co-JUGA)/o-MWCNT-modified electrodes were immersed into 500 μL of a solution containing 150 mM EDC + 300 mM NHS at 37°C for 2h to activate the carboxyl group. Then, electrodes were washed with distilled water and immersed into 500 μL of an aqueous solution containing 0.1 μM ODN probe for 2h at 37°C. Electrodes were then washed with MilliQ water and PBS at room temperature and immersed into PBS at 37°C under stirring for 2h to remove physisorbed ODN. After that, the electroactivity of poly(JUG-co-JUGA)/ODN- or poly(JUG-co-JUGA)/o-MWCNT/ODN-modified electrodes were investigated by SWV curves.

2.6. Hybridization assays

Hybridization solutions containing various concentrations of miRNA target (from 10^{-15} M up to 10^{-8} M) were prepared and heated for 5 minutes above the melting temperature of the corresponding duplex to avoid cross hybridization (Gortner et al., 1996; Válóczi et al., 2004). Probe-modified electrodes were then dipped into this solution at 45°C for 1h. After hybridization, electrodes were washed with 1xSSC (saline sodium citrate) buffer for 1 minute at 45°C then dipped into 1xPBS at 37°C for 30 min in order to wash out physisorbed targets. SWVs were then recorded in 1xPBS, at 25°C , several times consecutively until the signal is perfectly stable. The main peak (situated between -0.5 and -0.4 V vs. SCE) was used to calculate the relative current change (%ΔI/I) before and after hybridization, using the following equation:

$$\%\frac{\Delta I}{I} = \frac{I_{Hyb} - I_{Probe}}{I_{Probe}} \times 100$$

where I_{Probe} and I_{Hyb} are currents corresponding to the main SWV peak before and after hybridization, respectively.

The sample standard deviation was calculated as follows (Equation 1):

$$S = \sqrt{\frac{1}{(N-1)}\sum_{i=1}^{N}\left[\left(\frac{\Delta I}{I}\right)_i - \overline{\left(\frac{\Delta I}{I}\right)}\right]^2} \qquad \text{(Eq.1)}$$

with $\left(\frac{\Delta I}{I}\right)_i$ corresponding to the observed value of the relative current change for each measure *i* and $\overline{\left(\frac{\Delta I}{I}\right)}$ the mean value for N measurements.

The relative limit of detection $\left(\frac{\Delta I}{I}\right)_{LOD}$ was derived from the relative current change obtainedwith blank samples (Equation 2):

$$\left(\frac{\Delta I}{I}\right)_{LOD} = \overline{\left(\frac{\Delta I}{I}\right)}_{Blank} + 3S_{Blank} \qquad \text{(Eq. 2)}$$

with $\overline{\left(\frac{\Delta I}{I}\right)}_{Blank}$ corresponding to the mean value of the relative current change observed for blank samples and S_{Blank} the sample standard deviation for blank samples.

To obtain a calibration curve, at least three independent measurements were performed for each concentration. The limit of detection (LOD) was obtained from five independent blank samples.

2. Results and discussion

3.1. Electrode modifications and characterizations

The first step consists in the physisorption of a well-defined quantity of o-MWCNTs on the GC electrode surface. The procedure is detailed in the Experimental Section. Several surface densities of o-MWCNT were investigated: 0, 7, 14.3, 28.6, 36.7 and 142 µg cm^{-2} (see Fig. SI5). After that, poly(JUG-co-JUGA) was deposited by potential scans (20 scans) from 0.4 to 1.1 V (vs. SCE) at a scan rate of 0.05 V s^{-1}. The redox peaks situated at +0.91/+0.85 V vs. SCE develop continuously under scanning, which indicates formation of conducting poly(JUG-co-JUGA) film on the electrode surface. Fig. 1 shows CVs for a bare GC electrode (a) and for a o-MWCNT-modified electrode using 14.3 µg cm^{-2} (b). As expected, the currents measured on the o-MWCNT-modified electrode are higher than that on the bare GC one.

[insert Figure 1 here, single column]

(a)

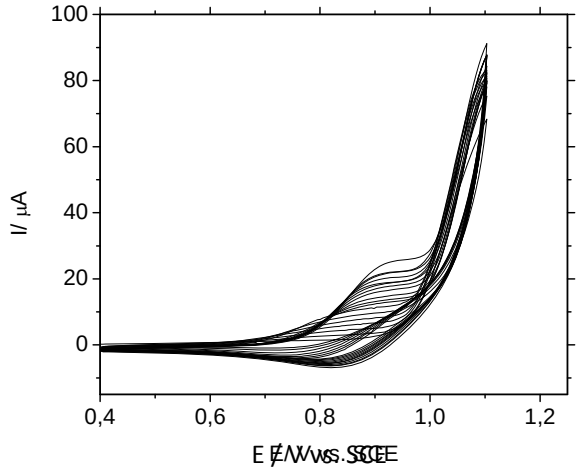

(b)

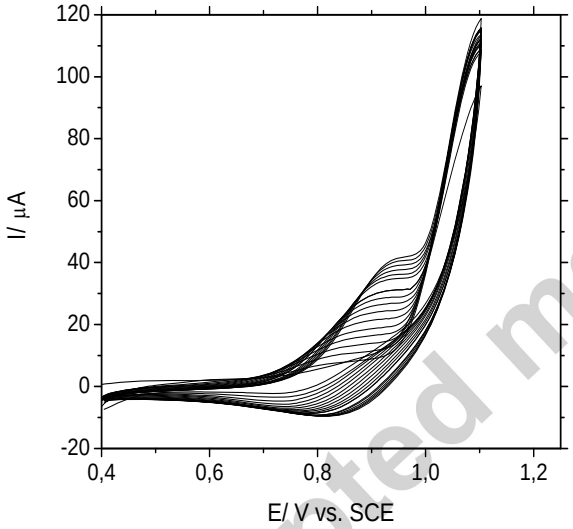

Figure 1

Fig. 2 shows FESEM pictures of (a) bare GC; (b) o-MWCNT/GC at low magnification; (c) o-MWCNT/GC at high magnification and (d) poly(JUG-co-JUGA)/o-MWCNT/GC. As shown, o-MWCNT-modified electrodes present much higher specific area than bare GC and, as expected, poly(JUG-co-JUGA) is deposited preferentially on the o-MWCNTs.

[Insert Figure 2 here; single column]

Figure 2

(a)

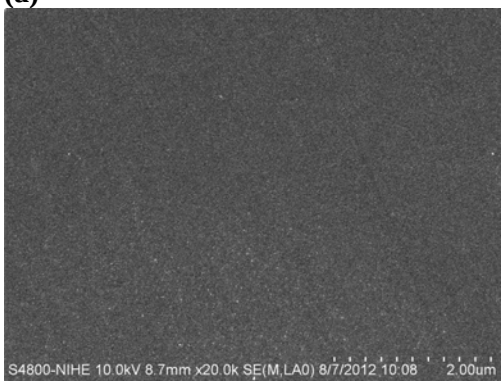

(b)

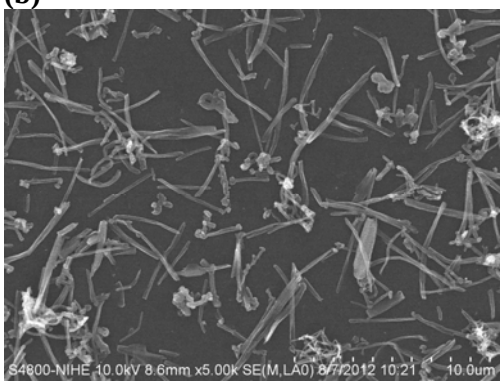

(c)

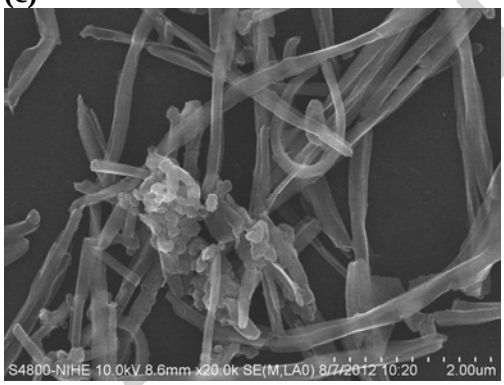

(d)

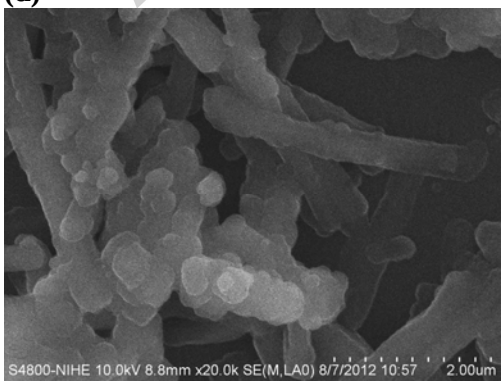

3.2. Electroactivity of the poly(JUG-co-JUGA)/o-MWCNT-modified electrodes

CVs of different polymer/o-MWCNT-modified electrodes are presented as supplementary information, Fig. SI1A. The higher the o-MWCNT density, the higher the current intensity, with a quasi-reversible signal observed in the cathodic potential domain between -1 and 0.1 V vs. SCE, attributed to quinone electroactivity. Two typical redox couples for quinone in PBS can be identified: a main couple is situated at -0.50/-0.65 V and a secondary one at -0.8/-0.85 V. Electrochemical impedance spectroscopy has been performed as well; results are given in Fig. SI1B.

Square wave voltammograms (SWV), which evidence the faradic peaks more clearly than CVs, are given on Fig. SI2. The o-MWCNT-modified electrode shows one small peak at -0.2 V vs. SCE, whereas the poly(JUG-co-JUGA)-modified electrode shows two well-defined peaks at -0.56 V vs. SCE (peak #1) and -082 V vs. SCE (peak #2) which correspond to the two quinone redox couples observed on the CVs. For the poly(JUG-co-JUGA)/o-MWCNT-modified electrode, peak #2 remains weak whereas peak #1 becomes predominant, along with a new shoulder (#3) at -0.32 V. Peak #3 increases with the o-MWCNT density (data not shown).

3.3. Detection of miRNA

ODN probes (ODN-141-P) were immobilized on poly(JUG-co-JUGA)/o-MWCNT-modified electrodes as described in the Experimental Section. The surface concentration Γ_{ODN} of ODN probe has been estimated around 10 ± 5 pmol cm^{-2} via fluorescence experiments after hybridization with fluorescent complementary target. Details are given as Supplementary Information. The maximum density Γ_{max} can be derived from the gyration radius R_G (R_G = 1.8 nm^2 for a single-stranded ODN of 22 bases) (Piro et al., 2007) which gives Γ_{max} = 17 pmol cm^{-2}. If ODN probe strands are closely packed on the electrode surface, this leads to a significant

steric hindrance which decreases the apparent diffusion coefficient of counter-ions, therefore decreases the current intensity of SWV. Conversely, hybridization leads to conformational reorganization of the double strands which creates free space on the electrode surface and induces a significant current increase (Reisberg et al., 2006; Piro et al., 2007).

miRNA of about the same length than the probes were used as targets (conditions are detailed in the Experimental Section and sequences are given in Table 1). Fig. 3a shows SWVs after hybridization with increasing concentrations of complementary miR-141 (10 fM, 1 pM, 100 pM). More curves are given on Fig. SI6. A complete calibration curve is given on Fig. 3b, where the relative current increase upon hybridization (%ΔI/I) is plotted versus the target concentration, in the range 10^{-15} M - 10^{-8} M. Saturation occurs beyond a concentration of 10^{-10} M; the limit of detection (LOD) is estimated around 8 fM (see Experimental Section). The linear part of the calibration curve corresponds to an extremely high sensitivity of +7.5 % per decade, which gives ΔI/I = 30 % for 10 pM miR-141. This is one of the lowest LOD reported for a reagentless and label-free electrochemical miRNA biosensor.

[Insert Figure 3 here; single column]

Figure 3

a)

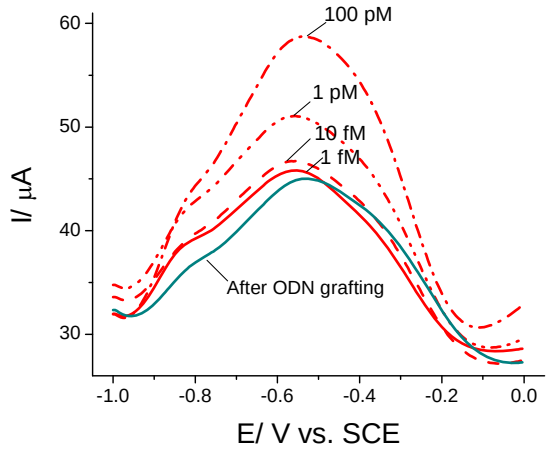

b)

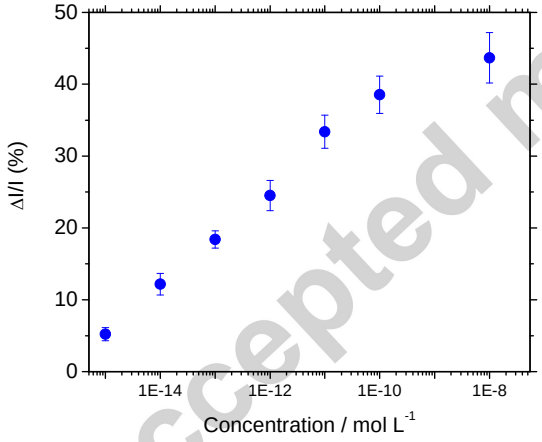

3.4. Selectivity of the sensor

To check the selectivity of the sensor, hybridization experiments were performed with two other non-complementary miRNAs: miR-103 and miR-29b-1 (see Table 1). Two concentrations were investigated, 1 pM and 10 pM (within the linear range determined from Fig. 3). As shown on Fig. SI3, the complementary target miR-141 leads to a current increase which is approximately three times higher than for the two non-complementary targets miR-103 and miR-29b-1. These results indicate that the biosensor is sufficiently selective to discriminate non-complementary miRNAs from the complementary one.

3-5 Detection of miRNA in diluted serum

The last set of experiments was conducted using human sera. A human normal serum (which does not contain miRNA in detectable quantity) was diluted fifty times and used as a blank; it is referred as 2% serum(-). From this solution were prepared samples in which known quantities of miR-141 were added, giving 2% serum(+) samples. A calibration curve is given on Fig. 4. Corresponding SWVs are given on Fig. SI4.

[Insert Figure 4 here; single column]

Figure 4

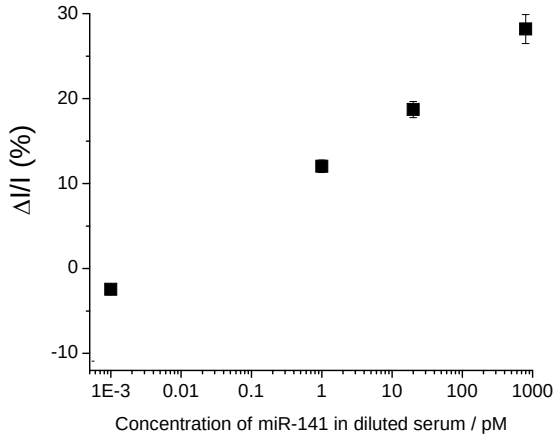

SWV performed on a 2% serum(-) solution led to a negative current change (decrease of the peak intensity) of about 10 %, which can probably be attributed to unspecific physisorption of serum proteins on the electrode surface (such solution contains around 1.5 mg mL^{-1} of various proteins). The current change is still negative for 10 fM (but yet significantly different from negative serum), which probably means that unspecific physisorption of proteins is predominant over the specific miRNA hybridization. For higher concentrations, the current change becomes positive, the LOD being significantly higher and the sensitivity lower than for experiments conducted in PBS instead of diluted serum.

3. Conclusion

A nanostructured poly(JUG-co-JUGA)/o-MWCNT composite was designed onto which oligonucleotide probes were grafted. The system was applied for direct electrochemical detection of miR-141, a miRNA biomarker. It is shown that the copolymer electroactivity is enhanced by the presence of o-MWCNTs, which probably participate to the low detection limit and high sensitivity. The sensor can work in complex samples such as diluted human serum. It is noteworthy to point out the interest to use *signal-on* transduction, which makes

the sensor much less sensitive to unspecific adsorption of proteins or nucleic acids than in case of *signal-off* transduction.

Work is now in progress to extent this detection system to use as probes PNA (peptide nucleic acids) or LNA (locked nucleic acids). These probes, having a higher affinity for RNA than DNA, are expected to attain even lower LOD and higher sensitivity.

Acknowledgements

H.V. Tran thanks the University of Sciences and Technology of Hanoi (USTH) for a PhD grant. The authors thank University Paris Diderot for financial support through an Interdisciplinary grant between Chemistry and Odontology Departments.

Figure and Table captions

Fig. 1. Cyclic voltammograms during film growth. Medium : 5.10^{-2} M JUG + 5.10^{-3} M JUGA + 10^{-3} M naphthol in ACN, a- on bare GC electrode; b- on o-MWCNT/GC using 14.3 µg cm^{-2} o-MWCNT.

Fig. 2. FESEM photographs on: (a) bare GC electrode; (b) o-MWCNT/GC at low magnification; (c) o-MWCNT/GC at high magnification (o-MWCNT density is 14.3 µg cm^{-2}) ; (d) poly(JUG-co-JUGA)/o-MWCNT/GC. Conditions: poly(JUG-co-JUGA) was deposited by 20 scans ; CNT's density is 14.3 µg cm^{-2}.

Fig. 3. a- SWVs recorded before adding miRNA-141(green curve) then after hybridization (red curves) with increasing concentrations of complementary miRNA-141: 1 fM, 10 fM, 1 pM and 100 pM. b- Calibration curve giving relative current increase (%ΔI/I) upon hybridization with concentrations of miRNA-141 in the range 10^{-15} M - 10^{-8} M.

Fig. 4. Calibration curve obtained from SWVs in 2% serum (-) and 2% serum (+), for 10 fM, 1 pM, 20 pM and 800 pM miR-141. Error bars were obtained by 3 independent experiments.

References

Acevedo, D.F., Reisberg, S., Piro, B., Peralta, D.O., Miras, M.C., Pham, M.C., Barbero, C.A., 2008. Electrochim. Acta 53, 4001-4006.

Brase, J. C., Wuttig, D., Kuner, R., Sültmann, H., 2010. Molecular Cancer 9, 306–313.

Cai, H., Xu, Y., He, P.G., Fang, Y.Z., 2003. Electroanalysis 15, 1864–1870.

Catuogno, S., Esposito, C.L., Quintavalle, C., Cerchia, L., Condorelli, G., De Franciscis, V., 2011. Cancers 3, 1877-1898.

Chen, H.Y, Lin, Y.M., Chung, H.C., Lang, Y.D., Lin, C.J., Huang, J., Wang, W.C., Lin, F.M., Chen, Z., Huang, H.D., Shyy, J.Y., Liang, J.T., Chen, R.H., 2012. Cancer Res. 72, 3631-3641.

Chen, X., Ba, Y., Ma, L., Cai, X., Yin, Y., Wang, K., Guo, J., Zhang, Y., Chen, J., Guo, X., Li, Q., Li, X., Wang, W., Zhang, Y., Wang, J., Jiang, X., Xiang, Y., Xu, C., Zheng, P., Zhang, J., Li, R., Zhang, H., Shang, X., Gong, T., Ning, G., Wang, J., Zen, K., Zhang J., Zhang, C.Y., 2008. Cell Res. 18, 997-1006.

Cosnier, S., 1999. Biosens. Bioelectron. 14, 443-456.

Cosnier. S., 2003. Anal. Bioanal. Chem. 377, 507–520.

Cosnier, S., Holzinger, M., 2011. Chem. Soc. Rev. 40, 2146-2156.

Fabbri, M., Garzon, R., Cimmino, A., Liu, Z., Zanesi. N, Callegari, E., Liu, S., Alder, H., Costinean, S., Fernandez-Cymering, C., Volinia, S., Guler, G., Morrison, C.D., Chan, K.K., Marcucci, G., Calin, G.A., Huebner, K., Croce, C.M., 2007. Proc. Natl. Acad. Sci. U.S.A. 104, 15805-15810.

Gao, Z., Peng, Y. 2011. Biosens. Bioelec. 26, 3768-3773.

Gerard, M., Chaubey, A., Malhotra, B.D., 2002. Biosens. Bioelectron. 17, 345–359.

Gortner, G., Pfenninger, M., Kahl, G., Weising, K., 1996. Electrophoresis 17, 1183-1189.

Hunt, A., Goulding, A. M., Deo. S. K., 2009. Anal. Biochem. 387, 1-12

Iorio, M.V. and Croce, C.M., 2009. J. Clin. Oncol. 27, 5848-5856.

Kilic, T., Topkaya, S.N., Ariksoysal, D.O., Ozsoz, M., Ballar, P., Erac, Y., Gozen, O., 2012. Biosens. Bioelec. 38, 195-201.

Kulesza, P.J., Skunik, M., Baranowska, B., Miecznikowski, K., Chojak, M., Karnicka, K., Frackowiak, E., B´eguin, F., Kuhn, A., Delville, M.H., Starobrzynska, B., Ernst, A., 2006. Electrochim. Acta 51, 2373-2379.

Lawrie, C. H., Gal, S., Dunlop, H. M., Pushkaran, B., Liggins, A. P., Pulford, K., Banham, A. H., Pezzella, F., Boultwood, J., Wainscoat, J. S., Hatton, C. S. R. and Harris, A. L., 2008. Br. J. Haematol. 141, 672-675.

Lee, R.C., Feinbaum, R.L., Ambros, V., 1993. Cell 75, 843–854.

Liu, X., He, S., Skogerbø, G., ong, F., Chen, R., 2012. PLoS ONE 7, e32797.

Lusi, E.A., Passamano, M., Guarascio, P., Scarpa, A., Schiavo, L., 2009. Anal. Chem. 81, 2819–2822

Mitchell, P.S., Parkin, R. K., Kroh, E. M., Fritz, B. R., Wyman, S. K., Pogosova-Agadjanyan, E. L. , Peterson, A., Noteboom, J., O'Briant, K. C., Allen, A., Lin, D. W., Urban, N., Drescher, C. W., Knudsen, B. S., Stirewalt, D. L., Gentleman, R., Vessella, R. L., Nelson, P. S., Martin, D. B., MTewari. Circulating microRNAs as stable blood-based markers for cancer detection, 2008. Proc. Natl. Acad. Sci. U.S.A. 105, 10513-10518.

Okuno, J., Maehashi, K., Kerman, K., Takamura, Y., Matsumoto, K., Tamiya, E., 2007. Biosens. Bioelectron. 22, 2377–2381.

Paleček, E. and Bartošík, M., 2012. Chem. Rev. 112, 3427-3481.

Peigney, A., Laurent, C., Flahaut, E., Bacsa, R. R., Rousset, A., 2001. Carbon 39, 507-514.

Peng, C., Jin, J., Chen, G.Z., 2007. Electrochim. Acta 53, 525-537.

Piro, B., Kapella, A., Hai, L.V., Anquetin, G., Zhang**,** Q.D., Reisberg, S., Noel, V., Tran, L.D., Duc, H.T., and Pham, M.C., 2011, Electrochim. Acta 55, 6136-6146

Piro, B., Reisberg, S., Noel, V., Pham, M.C., 2007. Biosens. Bioelectron. 22, 3126-3131.

Planell-Saguer, M. and Rodicio, M.C. Analytical aspects of microRNA in diagnostics: A review, 2011. Anal. Chim. Acta 699, 134-152

Qavi, A.J., Kindt, J.T., Bailey, R.C., 2010. Anal. Bioanal. Chem 398, 2535-2549

Qi, H., Li, X., Chen, P., Zhang, C., 2007. Talanta 72, 1030-1035.

Reisberg, S., Piro, B., Noel, V., Pham. M.C., 2006. Bioelectrochemistry 69, 172-179.

Shen, W., Deng, H., Ren, Y., Gao, Z., 2013. Biosens. Bioelec., DOI 10.1016/j.bios.2013.01.028.

Suni, I.I., 2008. Trends Anal. Chem. 27, 604-611

Válóczi, A., Hornyik, C., Varga, N., Burgyán, J., Kauppinen, S., Havelda, Z., 2004. Nucleic Acids Res. 32, e175.

Wang, J., 2005. Electroanalysis 17, 7–14.

Wang, J., Yi, X., Tang, H., Han, H., Wu, M., Zhou, F., 2012. Anal. Chem. 84, 6400-6406.

Wightman, B., Ha, I., Ruvkun, G., 1993. Cell 75, 855–862.

Wohlstadter, J.N., Wilbur, J.L., Sigal, G.B., Biebuyck, H.A., Billadeau, M.A., Dong, L., Fischer, A.B., Gudibande, S.R., Jameison, S.H., Kenten, J.H., Leginus, J., Leland, J.K., Massey, R.J. and Wohlstadter, S.J., 2003. Adv. Mater. 15, 1184–1187.

Xu, Y., Jiang, Y., Cai, H., He, P.G., Fang, Y.Z., 2004. Anal. Chim. Acta 516, 19–27.

Xu, Y., Ye, X.Y., Yang, L., He, P.A., Fang, Y.Z., 2006. Electroanalysis 18, 1471–1478.

Yin, H., Zhou, Y., Zhang, H., Meng, X., Ai, S., 2012. Biosens. Bioelec. 33, 247-253.

Zhang, G.J., Chua, J. H., Chee, R.E., Agarwal, A., Wong, S. M., 2009. Biosens. Bioelectron. 24, 2504–2508.

Zhang, Q. D., Piro, B., Noel, V., Reisberg, S., Pham, M. C., 2011. Analyst 136, 1023–1028.

Graphical Abstract

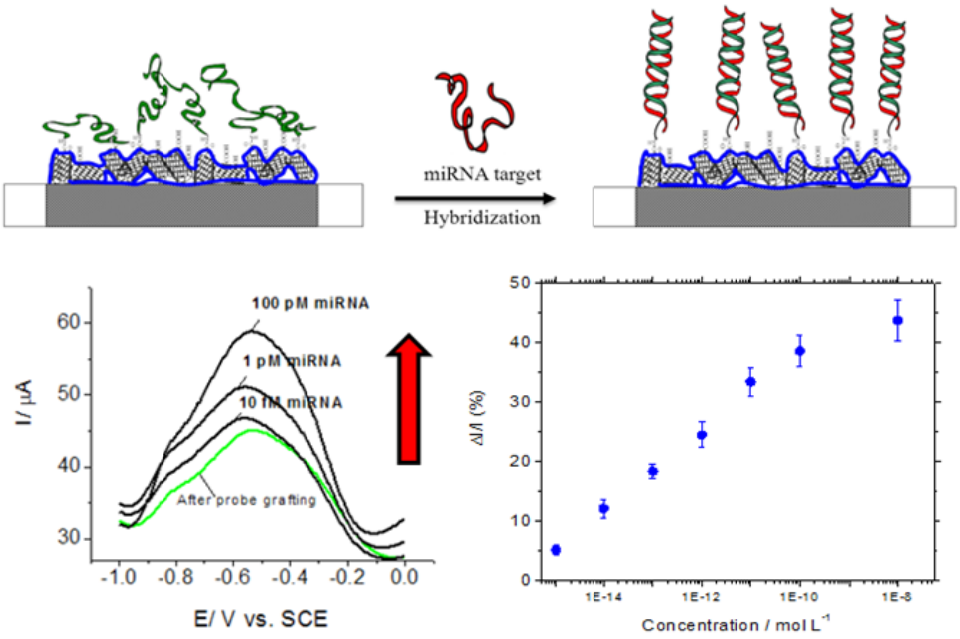

Highlights

►MicroRNA detection. ► Label-free and direct electrochemical detection. ► Conducting polymer nanostructured by carbon nanotubes. ► Prostate cancer biomarker miR-141